JURNAL INFOTEL
Informatics - Telecommunication - Electronics
Website Jurnal : http://ejournal.st3telkom.ac.id/index.php/infotel
ISSN : 2085-3688; e-ISSN : 2460-0997

Performance Analysis of Fetal-Phonocardiogram Signal Denoising Using The Discrete Wavelet Transform

Ipam Fuadina[1], Jans Hendry[2], Dodi Zulherman*[3]
[1] Fakultas Teknologi Industri dan Informatika, Institut Teknologi Telkom Purwokerto
[2, 3] Fakultas Teknik Telekomunikasi dan Elektro, Institut Teknologi Telkom Purwokerto
[1,2,3] Jl. D. I. Panjaitan, No. 128 Purwokerto 53147, Indonesia
*Corresponding email: zulherman.dodi@ittelkom-pwt.ac.id

Received 18 November 2019, Revised - , Accepted 16 December 2019

Abstract — The obligation for comprehensive fetal heart rate investigation had driven to improve the passive and non-invasive diagnostic instruments despite the USG or CTG method. Fetal phonocardiography (f-PCG) utilizing the auscultation method met the above criteria, but its interpretation frequently disturbed by the presence of noise. For instance, maternal heart and body organ sounds, fetal movements noise, and ambient noise from the environment where it is recording are the noise that corrupted the f-PCG signal. In this work, the use of discrete wavelet transforms (DWT) to eliminate noise in the f-PCG signal with SNR as the performance parameters observed. It was observing the effect of changes in wavelet type and threshold type on the SNR value. The test was carried out on f-PCG data taken from physio.net. Initial SNR values ranged from -26.7 dB to -4.4 dB; after application of DWT procedure to f-PCG, SNR increased significantly. Based on the test results obtained, wavelet type coif1 with the soft threshold gave the best result with 11.69 dB in SNR value. The coif1 had a superior result than other mother wavelets that use in this work, so the fPCG signal analysis for fetal heart rate investigation suggested to use it.

Keywords – fPCG, denoising, DWT, SNR, mother-wavelet

I. INTRODUCTION

Long-term observation of fetal heart rate (FHR) in the womb can be used to provide the health conditions of the fetus and mother required for pregnancy diagnosis. There are several generally known devices to diagnose fetal conditions, e.g., ultrasonography (USG), cardiotocography (CTG), and fetal-electrocardiography (f-ECG) [1], [2], [3]. The disadvantage of the use of USG or CTG for long-term observation is that the instrument is expensive, and well-skilled expertise is needed for obtaining and evaluating data. So, the more effective and more efficient device is needed to resolve such auscultation method [4]. The auscultation method uses an acoustic signal, a passive and non-invasive method, in the abdomen of maternal women to observe the pregnancy. Measurement of the acoustic signals in the abdominal area of maternal women can provide the FHR condition through recorded passive energy (known as the fetal-phonocardiography (fPCG) method) [2]. Typically, f-PCG has two fetal heart sounds, the first heart sound (S1) is produced by the closure of atrioventricular valves, and the second (S2) represents the closure of semilunar valves [4]. Considering its feature, f-PCG is a potential clinically useful test to evaluate fetal heart rate (FHR) during pregnancy and to assess fetal wellbeing during pregnancy, labor, and delivery [4]. However, f-PCG have an issue about the existence of other signals that coincide with the fetus heart sound such as maternal heart sounds (mHS), maternal organs sound (i.e., maternal digestion, respiratory movements), fetal movements, sensor movements, and ambient (environment) noise [5]. As it is heavily contaminated by noise, measurement fPCG using auscultation method implies mandatory to eliminate those signals from the fetus heart sound signal. Thus, appropriate filtering has to be applied in order to make fPCG clinically usable and to extract important diagnostic information, such as FHR [4].

The development of a method to eliminate noise on fPCG signals had been carried out by several researchers before. Varady et al. [2] showed the use of the wavelet method on two PCG channels and signal processing using the adaptive wavelet approach to obtain FHR. Kovacs et al. [6] developed the method that combines autocorrelation techniques, wavelet transforms, and matching pursuit to evaluate FHR. The use of other wavelet transform methods was carried out by Jaros et al. that observe wavelet performance compared to FIR [7]. In this work, the observation results of a discrete wavelet-based transformer noise (DWT) system by varying several wavelet-transform parameters such as wavelet type and threshold selection. Performance measurement was performed on the SNR value of the decomposed signal. Heriana and Misbah [8] stated that DWT has more advantages in the process of eliminating noise because it can analyze signals in the time domain and frequency domain simultaneously and can analyze in several structures. The present work explores wavelet transforms to reduce noise in fPCG signals. Performance observations were made of thirty-seven results of recording fPCG signals taken from physio.net secondary data providers [9][10].

II. RESEARCH METHOD

Denoising is the process of basic signal extracting from the mixed signals. Regardless of the frequency information content, all parts of the signal that are considered noise will be eliminated, so a new signal is obtained with the required features (such as S1 and S2 nodes in fPCG). The fPCG signal used in this study was taken from the Physionet.org website [11], which provides datasets that are quite complete and freely accessible. This data is called Simulated Fetal Phonocardiograms (simfpcgdb), which consists of 37 fPCG signals with details in Table 1 [12] that have been mixed with noise with SNR variations from -26.7 dB to -4.4 dB.

Table 1. Simfpcgdb Specification

Parameter	Description
SNR of noise	-26.7 dB - -4.4 dB
Sampling Rate	1 kHz
Resolution	16 bits
Gain	1

The fPCG signal is a signal of the measurement of fetal heart rate (non-invasive) through a maternal woman. It is a fetal heartbeat signal that is being conceived so that the mother's organs such as the skin mediate between the sensor and the fetus. There are several types of noise-producing activities for fPCG signals, namely [2] [14] maternal heart sounds (mHS), maternal organs sound (i.e., maternal digestion, respiratory movements), fetal movements, sensor movements, and ambient (environment) noise. Thus, the denoising procedures to obtain fPCG signal are required before a data from fPCG measurement results is analyzed, so that fPCG nodes such as S1 and S2 can be detected with high accuracy. In this research, a denoising process has been carried out using Discrete Wavelet Transform with variations of the mother wavelet to obtain the appropriate type of mother wavelet for denoising fPCG signals. The denoising system was developed using Matlab 2018a. Thus, the amplitude and sampling frequency information can be read directly by Matlab. In this work, the procedure of denoising fPCG signals is shown in Fig. 1. Meanwhile, the stages of the Signal Denoising process are shown by the flowchart in Fig. 2. To extract the fPCG signal, this work had several steps started by preprocessing using normalized and bandpass filter procedure. To make a threshold, the noise level estimation procedure had carried out and the next step was generating the global threshold used to denoising the process. After the denoising process, its performance was described by SNR values.

Signal denoising procedure is described in Fig. 2 that consists of three steps: forward wavelet transform, wavelet denoising, and inverse wavelet transform. The initial parameter for this procedure was obtained from the bandpass filtering process and the initial parameter that declares at the beginning, such as wavelet type, wavelet level, and threshold.

All fPCG signals were processed by employing a discrete wavelet transform (DWT). The fPCG signal of measurement results containing noise is defined by $x(n)$, the signal without noise is defined by $s(n)$, and the noise is symbolized by $\xi(n)$. The relationship between the three variables is expressed by (1).

$$x(n) = s(n) + \sigma\xi(n) \quad (1)$$

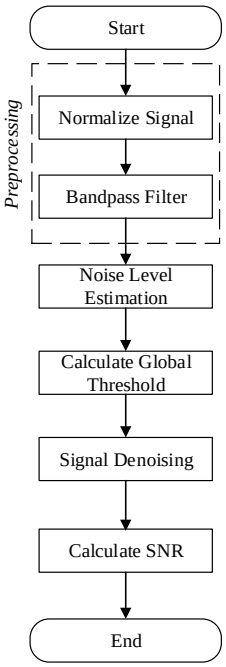

Fig.1. fPCG Signal Denoising Flowchart

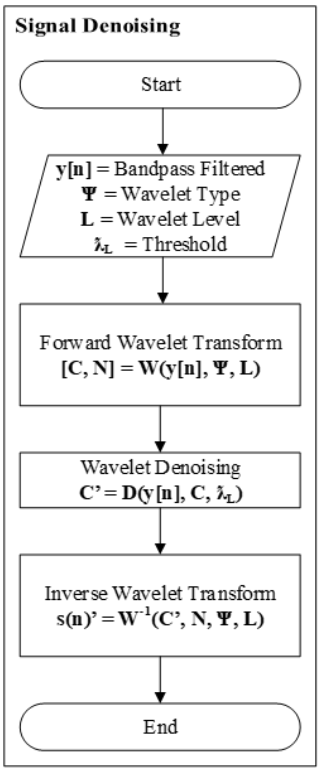

Fig. 2. Wavelet Denoising Flowchart

where σ is the noise level, the ξ(n) signal is a normally distributed random signal with an average of 0, and a standard deviation of 1 or is usually written as N (0, 1). The s(n) signal is the signal used in this study and then added with the noise ξ(n) to get the x(n) signal. By denoising, it is expected that the signal s(n) can be retrieved, which is symbolized by s^' (n) with the quality of the results measured based on the SNR parameter.

A. Preprocessing

The preprocessing phase was used to make the signal in the conditioning stage. The signal will sequentially process in two-step:

a) Normalize Signal

Firstly, the fPCG signal was normalized to get a signal in the range of -1 v to + 1 v. This process minimized the effect of anxiety signal amplitude. The fPCG signal was measured using sensors influenced by the activity of maternal and fetal organs. All of those activities were mixed in one recording/measurement that causes greater signal variability. For this reason, normalization was needed to reduce this variability. The normalization is defined as (2).

$$\tilde{x}[n] = x[n] / max(|x[n]|) \quad (2)$$

where $\tilde{x}[n]$ is a normalized signal. Although the simfpcgdb signal has been normalized, this step was a procedure always used as the beginning of processing.

b) Bandpass Filter

The noise in fPCG signals is usually below 20 Hz [13] (originating from the mother's internal organs) and above 70 Hz [2], [14], [15], [16] (originating from external factors). In research [17], the noise of your internal organs occupied a frequency of less than 25 Hz. Therefore, only certain frequency ranges will be taken using a bandpass filter. In this work, the Butterworth IIR bandpass filter was used which the filter order (M) was 10, and the frequency range corresponding to the simfpcgdb data was 30-80 Hz. This filter can also eliminate the influence of low frequency caused by signal bias (offset), so the expected value of the signal was 0. The frequency response of this filter is shown in Fig. 3 (a) and (b).

In Fig. 3 (a), the filter used to maintain the gain in the passband region (0 dB in the dotted line region), which means there is no change in the signal magnitude in the frequency range. While the signal outside the desired frequency range (stopband) has weakened to -50 dB. Through Fig. 3 (b), it appears that the phase shift is almost flat (flat) shown by the dotted line, which means that each frequency in the passband does not experience an angle shift.

Mathematically, the Butterworth IIR filter differential equation is formulated by (3).

$$y[n] = \sum_{i=0}^{M} a_i \tilde{x}[n-i] + \sum_{j=0}^{M} b_j\, y[n-j] \quad (3)$$

where y[n] is the filtering signal. Variables a_i and b_i, where i,j=0,1,…,M is the feedforward and feedback filter coefficients.

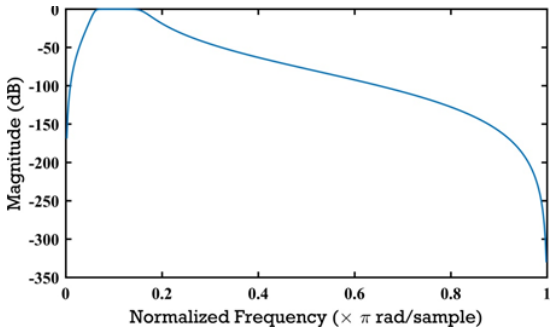

(a)

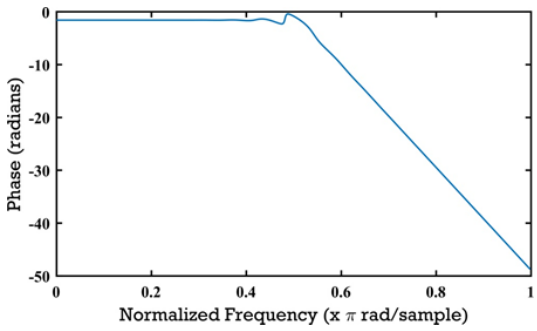

(b)

Fig. 3. Butterworth IIR Frequency Response (a) *Magnitude* (b) *Phase Shifts*

B. Noise Level Estimation

Thresholding in the wavelet transform was divided into two, namely global thresholding and level-dependent thresholding method. The thresholding process and its value make a difference between global and level-dependent thresholding. In the first method, the threshold value is calculated based on the entire data, including the threshold value. The second method, the threshold value, is different at each level (level), including the threshold carried out for each level. In this study, the method used was global thresholding.

Both methods involve the noise effect described in the noise level for the thresholding process. The noise level can be calculated with a statistical parameter such as standard deviation (σ), but it is not recommended because it requires the flat initial signal $s[n]$. In [18], another approach was shown for calculating the level of noise, as expressed in (4).

$$\tilde{\sigma} = \frac{med\{(|Q_n|):n=1,2,\ldots,N/2\}}{0.6745} \quad (4)$$

where $\tilde{\sigma}$ is the estimated noise level, Q_nis the coefficient of detail at the first level (finest level) wavelet decomposition. The aim of using the first level wavelet was that the noise composition at this level was more dominant than the level afterward. Assuming the most dominant noise was in the high-frequency spectrum, this coefficient was used in the calculation. Consistently with the fact, this coefficient was the result of the wavelet bandpass filter. To calculate the noise level in this study, we used the db1 mother wavelet type. If the data length of y[n] was N then the number of coefficients involved in this calculation was N/2 because the decomposition of the first level wavelet divides the signal into half of the original signal length.

C. Calculate Global Threshold (Calculate Global Threshold)

Determining the threshold values are used by the Universal Rule principle [19] expressed as (5).

$$\lambda_L = \tilde{\sigma}\sqrt{2\,log(N)} \quad (5)$$

λ_L is the threshold value calculated based on the level of noise that had been found through (4)? When the signal was normalized to the noise deviation standard, the variability of noise level was nonessential value. This threshold value was used for all wavelet detail coefficients.

D. Signal Denoising

The denoising process using wavelets consists of several stages:

a) Feedforward Wavelet Transform

The noisily fPCG signal $y[n]$ was processed to wavelet transformation with decomposition level (L) was four, and mother wavelets were Daubechies, Symlets, Coiflets family. The aim of choosing the type of mother wavelet was the investigation of the most suitable for denoising in this study. These three wavelet families were chosen because they are most suitable for denoising adult [20] and fetus signals [21], [22]. Wavelet as a filter bank consists of a low pass filter (LPF) and a high pass filter (HPF). The output of LPF was the approximation coefficient (cA), while the output of HPF was the coefficient of detail (cD). The relationship between the two groups of coefficients was illustrated by (6).

$$\hat{y}[n] = \sum_{m\in\mathbf{Z}} cA_J[m]\Phi_{J,m}[n] + \sum_{m\in\mathbf{Z}}\sum_{j=1}^{J} cD_j[m]\Psi_{j,m}[n] \quad (6)$$

where $\Phi_{J,m}$ was a scaling function and $\Psi_{j,m}$ was a wavelet function. The Zahlen symbol ($\mathbb{Z}$), indicated the set of integers and $\hat{y}[n]$ was the result of a wavelet transformation. Variables j and k indicate scale and position.

Noise usually occupies the high-frequency spectrum, so the denoising process was carried out in this region. Using the 3dB-frequency was 30-80 Hz, whereas the sampling frequency was 1 kHz. By following the Nyquist theory, the maximum frequency of fPCG recordings was 500 Hz. Respectively value of these frequencies, the value above 80 Hz, can be said as the high-frequency spectrum.

b) Denoising

In this study, the denoising process was applied for all the detail coefficients (cD) of wavelet decomposition products. Besides the approximation coefficient (cA) was processed only for the last level coefficient *J*. The threshold value used was λ_L and applied to all levels of decomposition, which was also called the independent thresholding level [19]. The threshold technique used consists of 2 namely hard thresholding and soft thresholding. The hard thresholding technique based on one threshold value shown by (7) [19].

$$D_H^{\lambda_L}\left(cD_{j,\ldots,J}\right) \equiv \begin{cases} cD_{j,\ldots,J} & for\ all\ |cD| > \lambda_L \\ 0 & otherwise \end{cases} \quad (7)$$

Variables $D_H^{\lambda_L}$ were the result of a threshold. Based on this threshold, the initial detail coefficient value keep up if it exceeds the threshold value. As for soft thresholding floating techniques expressed by (8) [10].

$$D_S^{\lambda_L}\left(cD_{j,\ldots,J}\right) \equiv \mathrm{sgn}\left(cD_{j,\ldots,J}\right)\max\left(0;\left|cD_{j,\ldots,J}\right| - \lambda_L\right) \quad (8)$$

The variable $D_S^{\lambda_L}$ was the threshold value from the soft thresholding technique where $\mathrm{sgn}\left(cD_{j,\ldots,J}\right)$ as a positive or a negative sign for detail coefficient. The difference between the first technique and the second technique was illustrated in Fig. 4.

c) Inverse forward wavelet transform

Based on the previous section, only the detail coefficient had implemented threshold, the signal reconstruction ($s'[n]$) at the end of the process was expressed by (9).

$$s'[n] = cA_J[n] + \sum_{j=1}^{J} cD_j[n] \quad (9)$$

the reconstruction output was a combination of all the thresholding output of detailed coefficients at each level decomposition and the coefficient of approximation at the last level of decomposition.

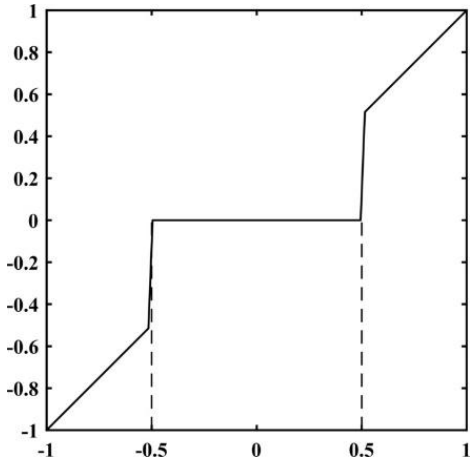

(a)

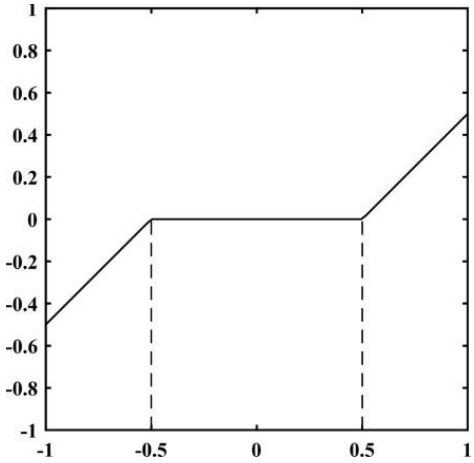

(b)

Fig. 4. Comparison of Thresholding Method, (a) Hard Thresholding, (b) Soft Thresholding

E. Signal to Noise Ratio

The denoising system performance was measured through Signal to Noise Ratio (SNR). In [11] did not provide the original signal contaminated by noise, so it was difficult to compare the denoising signal to the reference signal. Because of the absence of the reference signal, SNR is calculated using the mathematical expression used by [23] in (10).

$$SNR = 20\log_{10}\left(\frac{s'_{p-p}[n]}{4\sigma(s'[n])}\right)dB \quad (10)$$

where the parameter $\sigma(s'[n])$ was the standard deviation of the reconstruction signal and the value $s'_{p-p}[n]$ was the peak to peak signal $s'[n]$.

III. RESULT

The fPCG signal used in this study was a simulated fPCG signal (simfpcgdb) with a total of 37 signals mixed noise with SNR variations. These signals were implemented in the denoising process following the stages that have been designed. In Fig. 5, an fPCG signal with the file name **fetalPCG_simulatedSNR-8_1dB** recorded at a sampling frequency (*fs*) = 1 kHz and duration of 30 seconds. In this figure, we just showed the data for the 1-second duration to facilitate observation in the time zone.

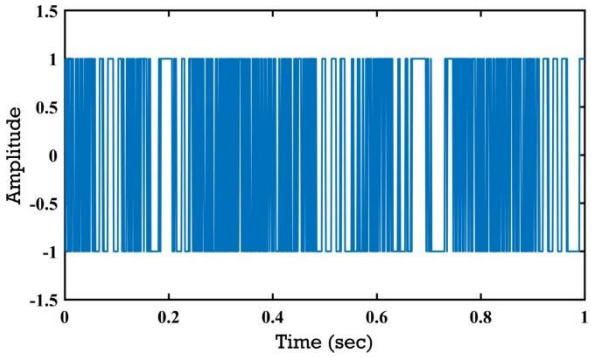

Fig. 5. fetalPCG_simulatedSNR-8_1dB signal

The simfpcgdb data was downloaded online and automatically using the wfdb toolbox [24]. The downloaded signal looks like a coherence normalized rectangular signal. Based on the Fourier theory, a summary of infinite number signal with different frequencies will form a square signal when it was added, so it is very reasonable when the signal was charged with a bandpass filter at the initial stage. A Butterworth IIR filter has been designed to filter the signal so that it produces the signal in Fig. 6.

The output signal from the IIR filter showed a different signal from the original one. Even, Fig. 6 displayed some vertices S1 and S2, but there are still high-frequency components that need to be attenuate or remove. After the noise removing, the transitions between nodes (S1 to S2 or S2 to S1) became clearer. For this reason, wavelet transformation was used at the denoising stage.

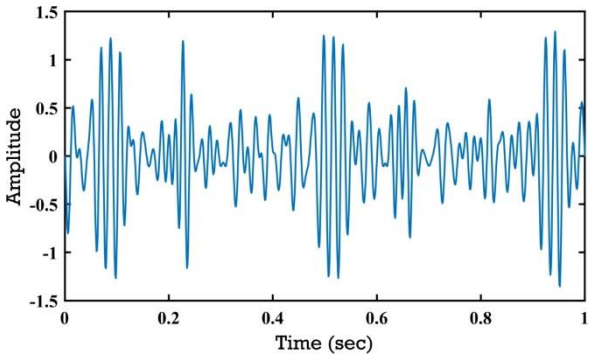

Fig. 6. The Output of IIR Butterworth Bandpass Filter

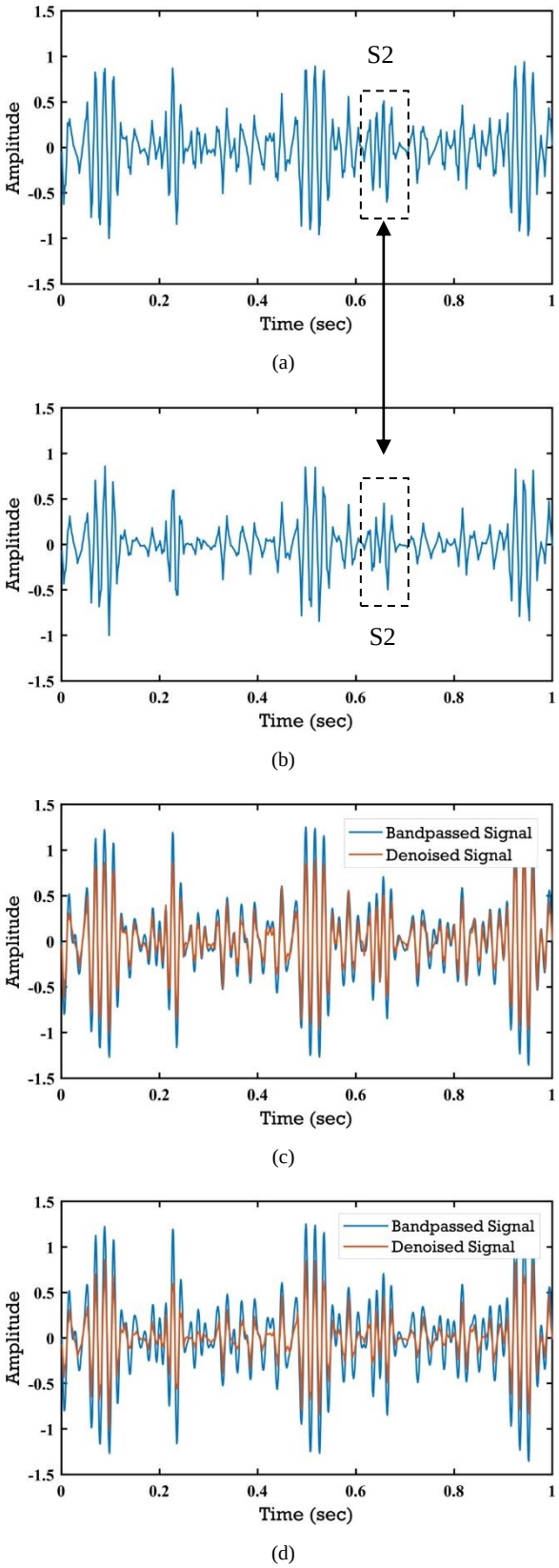

Fig. 7. Denoising Signal (a) Hard Thresholding, (b) Soft Thresholding, (c) Bandpass Filter vs. Hard Thresholding, (d) Bandpass Filter vs. Soft Thresholding

Fig. 7 shows the comparison of fPCG signals after reconstruction using the two threshold techniques and the comparison with the results of the Butterworth IIR bandpass filter. In the time domain, the results of soft thresholding were smoother than hard thresholding in some parts of the signal. It happened because the non-zero value of the detail coefficient had changed mathematically in soft thresholding while it not happened in hard thresholding. The area that highlights with a box in Fig. 7 shows the signal part that was still clear on the hard thresholding results, but it attenuates in the soft thresholding result. However, soft thresholding was always better than hard thresholding because the aims of denoising fPCG signals and other biomedical signals were not only to eliminate noise but also to produce new representations of signals such as the clarity of the position of S1 and S2 signals. The use of soft thresholding tended to weaken the signal power, so S2 became vulnerable to losses due to shrinkage, which did not occur in the hard thresholding, as shown by the two-way arrows in Fig. 9 (a) and (b).

IV. DISCUSSION

There were ten types of wavelets from 3 different families used in this study, namely db4, db5, db7, db10, sym5, sym7, sym10, coif1, coif2, and coif4. The IIR filter output of 37 fPCG data was decomposed to the 4th level.

For the next stage, the SNR parameters were calculated for each decomposed signal reconstructed by the wavelet transform with different mother wavelet types and the thresholding method. The results of the SNR parameters are shown in Fig. 8.

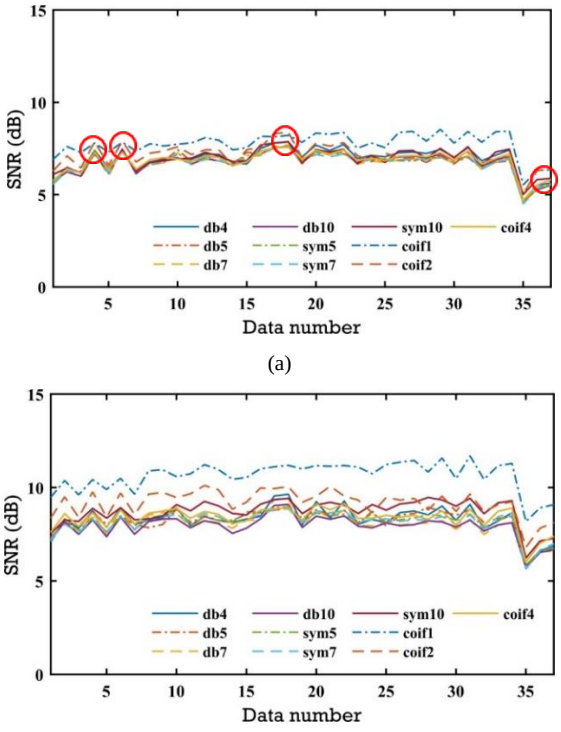

Fig. 8. SNR Value from Different Mother Wavelet and Thresholding Method, (a) Hard Thresholding, (b) Soft Thresholding

Based on Fig. 8, it can be concluded that the type of wavelet that had the largest SNR was coif1 from the coiflet family. The best SNR value for this wavelet type was 8,5365 dB for the hard thresholding and 11.6940 dB for the soft thresholding. Even though in Fig. 6 (a), the coif2 wavelet type had a better SNR value about four times, which is circled in red than coif1, but principally the coif1 had better SNR value than coif2. Hence, the coif1 mother wavelet was used as a wavelet type to reconstruct the denoising signal in the next discussion.

The coefficient of detail at all levels before and after the threshold was shown in Fig. 9. The two-way arrow in Fig.9 showed a sample of significant differences between the results of hard thresholding and soft thresholding. It was caused by the amplitude of the reconstruction signal from soft thresholding smaller than the hard thresholding. Hence, a combination of the highest levels approximation coefficient gave the smoother signal (not jaggy) in some samples.

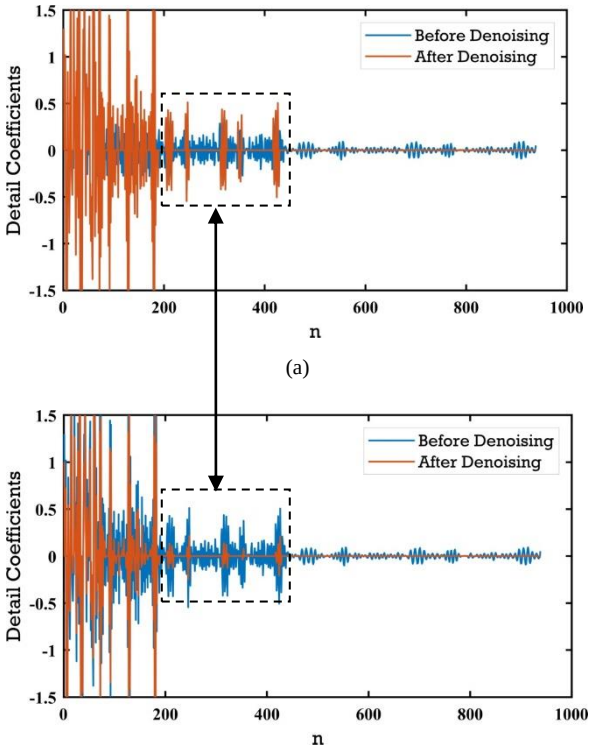

Fig. 9. Detail Coefficient Before and After Denoising (a) Hard Thresholding, (b) Soft Thresholding

The filtering output can also be observed through the frequency spectrum. In Fig. 10 (a) - (d), the frequency spectrum of the original fPCG signal, and after the denoising process were displayed. The original fPCG signal spectrum contained a very dense and distributed frequency spectrum in the range of 0 - 500 Hz, shown in Fig. 10 (a). The filtering process also proved the previous explanation related to the basic principles of Fourier analysis. By using the Butterworth IIR bandpass filter, only the frequency spectrum in the range 30 - 80 Hz was passed. There was almost no frequency leak (spectrum leakage), as in Fig. 10 (b).

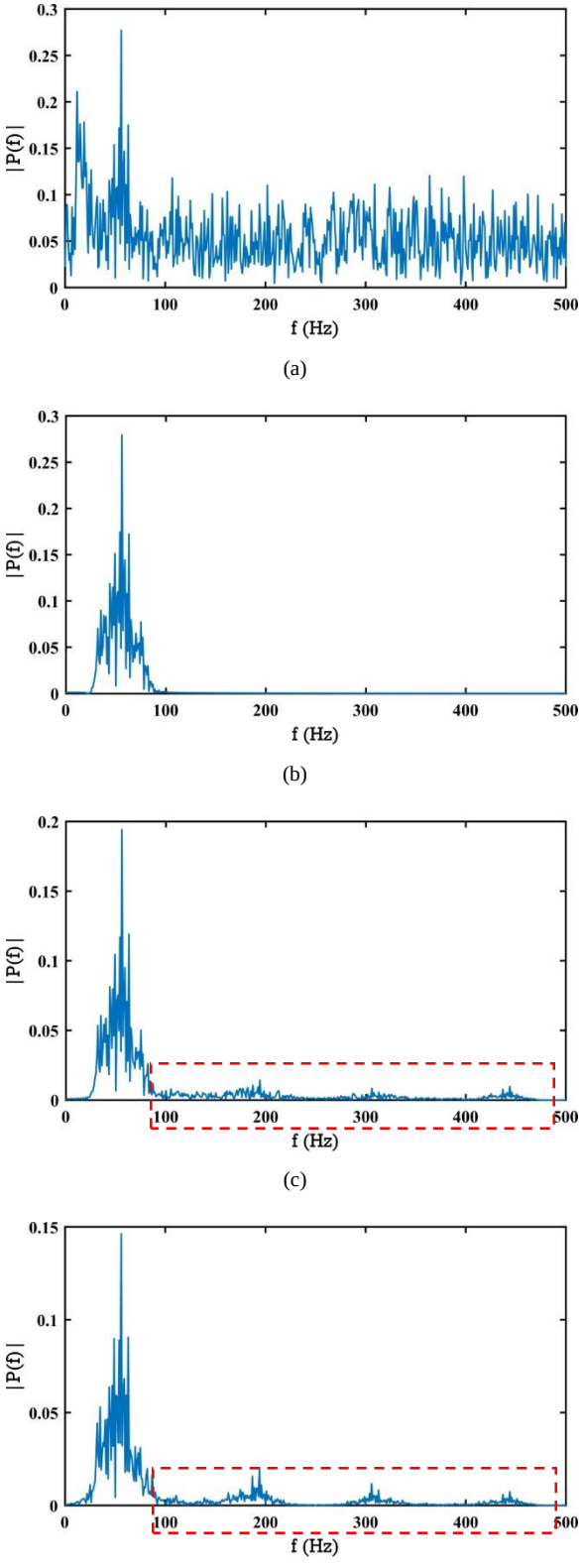

Fig.10. fPCG Spectrum (a) Original Signal, (b) Bandpass Filtering, (c) Hard Thresholding, (d) Soft Thresholding

The interesting results were the distribution of the frequency spectrum after denoising by hard thresholding and soft thresholding. As shown in the frequency spectrum in Fig. 10 (c) and (d), the frequency spectrum appears above 80 Hz, which was almost flat. The magnitude is indeed not too large compared to the fundamental frequency and harmony, but this confirms that the thresholding process carried out on all the coefficients of detail greatly affects the high-frequency spectrum. This is very reasonable (reasonable) because the coefficient of detail is the result of filtering the wavelet high-frequency escaping filter. When the coefficient values change - which was already in a certain frequency range - resulting in the creation of another high-frequency spectrum, which is also called a frequency leakage (frequency leakage). The spectrum can be removed by setting a certain threshold value (hard thresholding) as part of post-processing but requires more in-depth and thorough research. Also, through this frequency spectrum, it can be concluded that the hard and soft thresholding techniques result in a weakening of the IIR filter spectrum. Frequency leakage resulting from soft thresholding is greater than hard thresholding because almost all of the detail coefficient values experience changes in value that are not experienced by hard thresholding.

V. CONCLUSION

The denoising process using wavelets was carried out in this study. A total of 10 types from three wavelet families had been tested to determine the proper type in terms of SNR values. Based on the results, mother wavelet coif1 from the coiflet family produced the best SNR value of 8,5365 dB for hard thresholding and 11.6940 dB for soft thresholding. This wavelet type dominated the largest SNR value compared to other wavelet types, including the other coiflet family. This wavelet type was recommended to use in fPCG signal analysis especially in the denoising process, to get the S1 and S2 nodes that are useful for calculating FHR (Fetal Heart Rate).

ACKNOWLEDGMENT

The authors would like to express our sincere gratitude to LPPM Institut Teknologi Telkom Purwokerto for providing their assistance in the research administration. Authors would specially thank Kementerian Riset, Teknologi, dan Pendidikan Tinggi (Kemenristekdikti) Republik Indonesia as research funder (Skema Penelitian Dosen Pemula).

REFERENCES

[1] E. Koutsiana, L. J. Hadjileontiadis, I. Chouvarda, and A. H Khandoker, "Detecting fetal heart sounds by means of fractal dimension analysis in the wavelet domain," in *Annual International Conference of the IEEE Engineering in Medicine and Biology Society*, Soegwipo, 2017

[2] P. Varady, L. Wildt, Z. Benyo, and A. Hein, "An advanced method in fetal phonocardiography," *Computer methods and programs in biomedicine*, vol. 71, no. -, pp. 283-296, 2003

[3] L. J. Spyridou, "Analysis of fetal heart rate in healthy and pathological pregnancies using wavelet-based featureí," in *Annual International Conference of the IEEE EMBS*, Lyon, 2007

[4] A. Sbrollini et. al., "Fetal phonocardiogram denoising wavelet transformation: robustness to noise," *Computing in Cardiology*, vol. 44, no. -, pp. 1-4, 2017

[5] D. Gradolewski, G. Redlarski, "Wavelet-based denoising method for real phonocardiography signal recorded by mobile devices in a noisy environment," *Computers in Biology and Medicine*, vol. 52, no. -, pp. 64-70, 2011

[6] F. Kovacs, C. Horvath, A. T. Balogh, and G. Hosszu, "Extended noninvasive fetal monitoring by detailed analysis of data measured with phonocardiography," *IEEE Transaction on Biomedical Engineering*, vol. 58, no. 1, pp. 64-70, 2011

[7] R. Jaros, R. Martinek, R. Kahankova, M. Fajkus, and J. Nedoma, "Comparison of fetal phonocardiogram de-noising by wavelet transform and the FIR filter," in *2018 IEEE 20th International Conference on e-Health Networking, Applications and Services (Healthcom)*, Ostrava, 2018

[8] O. Heriana, A. M. A. Misbah, "Perbandingan unjuk kerja transformasi *wavelet* dalam *denoising* sinyal ECG," *Jurnal Elektronika dan Telekomunikasi (JET)*, vol. 17, no. 1, pp. 1-6, 2017

[9] M. Samieinasab dan R. Sameni, "Fetal phonocardiogram extraction using single-channel blind source separation," in *23rd Iranian Conference on Electrical Engineering*, Tehran, 2015

[10] C. Liu, D. Springer, Q. Li, B. Moody, R. A. Juan, F. J. Chorro, F. Castells, J. M. Roig, I. Silva, and A. E. W. Johnson, "An open-access database for the evaluation of heart sound algorithms," *Physiological Measurement*, vol. 37, no. 12, pp.2181-2213, 2016

[11] A. L. Goldberger et al., "PhysioBank, PhysioToolkit, and PhysioNet: Components of a New Research Resource for Complex Physiologic Signals," *Circulation*, 101(23):e215-e220, 2003.

[12] M. Cesarelli, M. Ruffo, M. Romano, and P. Bifulco, "Simulation of foetal phonocardiographic recordings for testing of FHR extraction algorithms," *Comput Methods Programs Biomed*, 107(3):513-23, September 2012.

[13] M Ruffo, M. Cesarelli, C. Jin, G. Gargiulo, A. McEwan, C. Sullivan, P. Bifulco, M. Romano, R. W. Shephard, and A. v. Schaik, "Non-Invasive Foetal Monitoring with Combined ECG - PCG System," In book: *Biomedical Engineering, Trends in Electronics, Communications, and Software*, 2011.

[14] A. K. Mittra, N. K. Choudhary, and A. S. Zadgaonkar, "Development of an artificial womb for acoustical simulation of mother's abdomen," *Int. J. Biomedical Engineering and Technology*, Vol. 1, No. 3.

[15] H. E. Bassil and J.H. Dripps, "Real-time processing and analysis of fetal phonocardiographic signals," *Clin. Phys. Physiol. Meas.*, Vol. 10, Suppl. B, 67 - 74, 1989.

[16] F. Kovacs, M. Torok, and I. Habermajer, "A rule-based phonocardiographic method for long-term fetal heart rate monitoring," *IEEE Trans. on Biomed. Eng.*, vol. 47, no 1, January 2000.

[17] F. Kovács, C. Horváth, Á. T. Balogh, and G. Hosszú, "Fetal phonocardiography-Past and future possibilities," *Computer methods and programs in biomedicine*, 104, pp. 19 - 25, 2011.

[18] D. Donoho and I. Johnstone, "Adapting to unknown smoothness via wavelet shrinkage," *Journal of the American Statistical Association*, 90: 1200 - 1 224, 1995.

[19] K. P. Soman, K. I. Ramachandran, and N. G. Resmi, "Insight Into Wavelets From Theory to Practice," in *PHI Learning, 3rd ed*, 2010.

[20] S. R. Messer, J. Agzarian, and D. Abbottt, "Optimal wavelet denoising for phono-cardiograms," *Microelectron. J.* 32 (2001) 931 - 941.

[21] Y. Song, W. Xie, J. F. Chen, and K. S. Phua, "Passive acoustic maternal abdominal fetal heart rate monitoring using the wavelet transform," *Comput. Cardiol*. 33 (2006) 581–584 (September).

[22] P. Varady, "Wavelet-based adaptive denoising of phonocardiographic records," in: *Proceedings of the 23rd Annual Engineering in Medicine and Biology Society International Conference*, Istanbul, Turkey, 2001, pp. 1846 - 1849.

[23] A. Sbrollini, A. Strazza, M. Caragiuli, C. Mozzoni, S. Tomassini, A. Agostinelli, M. Morettini, S. Fioretti, F. D. Nardo, and L. Burattini, "Fetal Phonocardiogram Denoising by Wavelet Transformation: Robustness to Noise," *Computing in Cardiology*, Vol 44, 2017.

[24] Physionet, wfdb toolbox. [Online]. Available: https://physionet.org/physiotools/matlab/ wfdb-app-matlab/